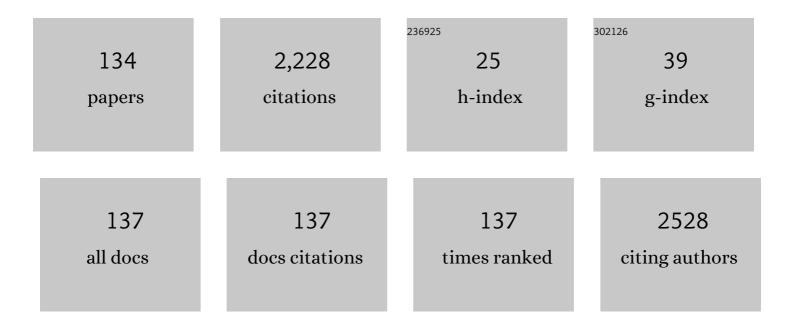
List of Publications by Year in descending order

Source: https://exaly.com/author-pdf/9441672/publications.pdf Version: 2024-02-01



#	Article	IF	CITATIONS
1	Basis of FLT as a cell proliferation marker: comparative uptake studies with [3H]thymidine and [3H]arabinothymidine, and cell-analysis in 22 asynchronously growing tumor cell lines. Nuclear Medicine and Biology, 2002, 29, 281-287.	0.6	100
2	Basic characterization of 64Cu-ATSM as a radiotherapy agent. Nuclear Medicine and Biology, 2005, 32, 21-28.	0.6	93
3	α7 Nicotinic Receptor Agonists: Potential Therapeutic Drugs for Treatment of Cognitive Impairments in Schizophrenia and Alzheimer's Disease~!2009-10-15~!2009-10-30~!2010-05-27~!. Open Medicinal Chemistry Journal, 2010, 4, 37-56.	2.4	85
4	Preclinical and the first clinical studies on [11C]CHIBA-1001 for mapping α7 nicotinic receptors by positron emission tomography. Annals of Nuclear Medicine, 2009, 23, 301-309.	2.2	75
5	Comparison between new-generation SiPM-based and conventional PMT-based TOF-PET/CT. Physica Medica, 2017, 42, 203-210.	0.7	73
6	High occupancy of σ1 receptors in the human brain after single oral administration of donepezil: a positron emission tomography study using [11C]SA4503. International Journal of Neuropsychopharmacology, 2009, 12, 1127.	2.1	63
7	Changes in Cerebral Blood Flow during Steady-State Cycling Exercise: A Study Using Oxygen-15-Labeled Water with PET. Journal of Cerebral Blood Flow and Metabolism, 2014, 34, 389-396.	4.3	61
8	α7 Nicotinic Receptor Agonists: Potential Therapeutic Drugs for Treatment of Cognitive Impairments in Schizophrenia and Alzheimer's Disease. Open Medicinal Chemistry Journal, 2010, 4, 37-56.	2.4	56
9	[11C]Gefitinib ([11C]Iressa): Radiosynthesis, In Vitro Uptake, and In Vivo Imaging of Intact Murine Fibrosarcoma. Molecular Imaging and Biology, 2010, 12, 181-191.	2.6	54
10	Feasibility studies of 4′-[methyl-11C]thiothymidine as a tumor proliferation imaging agent in mice. Nuclear Medicine and Biology, 2008, 35, 67-74.	0.6	52
11	Imaging of Sigma1 Receptors in the Human Brain Using PET and [11C]SA4503. Central Nervous System Agents in Medicinal Chemistry, 2009, 9, 190-196.	1.1	49
12	4′-[Methyl- ¹¹ C]-Thiothymidine PET/CT for Proliferation Imaging in Non–Small Cell Lung Cancer. Journal of Nuclear Medicine, 2012, 53, 199-206.	5.0	43
13	Comparison of 11C-4′-thiothymidine, 11C-methionine, and 18F-FDG PET/CT for the detection of active lesions of multiple myeloma. Annals of Nuclear Medicine, 2015, 29, 224-232.	2.2	42
14	Direct comparison of radiation dosimetry of six PET tracers using human whole-body imaging and murine biodistribution studies. Annals of Nuclear Medicine, 2013, 27, 285-296.	2.2	39
15	Whole-Body Distribution and Brain Tumor Imaging with ¹¹ C-4DST: A Pilot Study. Journal of Nuclear Medicine, 2011, 52, 1322-1328.	5.0	38
16	Trends in nucleoside tracers for PET imaging of cell proliferation. Nuclear Medicine and Biology, 2003, 30, 681-685.	0.6	36
17	Regional Cerebral Glucose Metabolism and Gait Speed in Healthy Community-Dwelling Older Women. Journals of Gerontology - Series A Biological Sciences and Medical Sciences, 2014, 69, 1519-1527.	3.6	35
18	Initial Human PET Studies of Metabotropic Glutamate Receptor Type 1 Ligand 11C-ITMM. Journal of Nuclear Medicine, 2013, 54, 1302-1307.	5.0	34

#	Article	IF	CITATIONS
19	Evaluation of 4'-[methyl-14C]thiothymidine for in vivo DNA synthesis imaging. Journal of Nuclear Medicine, 2006, 47, 1717-22.	5.0	33
20	Recent Development of Radioligands for Imaging α7 Nicotinic Acetylcholine Receptors in the Brain. Current Topics in Medicinal Chemistry, 2010, 10, 1544-1557.	2.1	32
21	In Vivo Evaluation of α7 Nicotinic Acetylcholine Receptor Agonists [11C]A-582941 and [11C]A-844606 in Mice and Conscious Monkeys. PLoS ONE, 2010, 5, e8961.	2.5	31
22	Biodistribution and radiation dosimetry of the $\hat{I}\pm7$ nicotinic acetylcholine receptor ligand [11C]CHIBA-1001 in humans. Nuclear Medicine and Biology, 2011, 38, 443-448.	0.6	31
23	Brain histamine H ₁ receptor occupancy measured by PET after oral administration of levocetirizine, a non-sedating antihistamine. Expert Opinion on Drug Safety, 2015, 14, 199-206.	2.4	31
24	Occupancy of adenosine A2A receptors by istradefylline in patients with Parkinson's disease using 11C-preladenant PET. Neuropharmacology, 2018, 143, 106-112.	4.1	29
25	Characterization of [3H]CHIBA-1001 binding to α7 nicotinic acetylcholine receptors in the brain from rat, monkey, and human. Brain Research, 2010, 1348, 200-208.	2.2	27
26	Regional analysis of striatal and cortical amyloid deposition in patients with <scp>A</scp> lzheimer's disease. European Journal of Neuroscience, 2014, 40, 2701-2706.	2.6	26
27	Long-term cilostazol administration ameliorates memory decline in senescence-accelerated mouse prone 8 (SAMP8) through a dual effect on cAMP and blood-brain barrier. Neuropharmacology, 2017, 116, 247-259.	4.1	26
28	Occupancy of α7 Nicotinic Acetylcholine Receptors in the Brain by Tropisetron: A Positron Emission Tomography Study Using [11C]CHIBA-1001 in Healthy Human Subjects. Clinical Psychopharmacology and Neuroscience, 2011, 9, 111-116.	2.0	25
29	Advances in the Development of PET Ligands Targeting Histone Deacetylases for the Assessment of Neurodegenerative Diseases. Molecules, 2018, 23, 300.	3.8	24
30	Rationale of 5-(125)I-iodo-4'-thio-2'-deoxyuridine as a potential iodinated proliferation marker. Journal of Nuclear Medicine, 2002, 43, 1218-26.	5.0	24
31	Cerebral Acetylcholinesterase Imaging: Development of the Radioprobes. Current Topics in Medicinal Chemistry, 2007, 7, 1790-1799.	2.1	23
32	Initial Evaluation of an Adenosine A _{2A} Receptor Ligand, ¹¹ C-Preladenant, in Healthy Human Subjects. Journal of Nuclear Medicine, 2017, 58, 1464-1470.	5.0	23
33	Potential Use of 18F-THK5351 PET to Identify Wallerian Degeneration of the Pyramidal Tract Caused by Cerebral Infarction. Clinical Nuclear Medicine, 2017, 42, e523-e524.	1.3	23
34	Development of radioiodinated nucleoside analogs for imaging tissue proliferation: comparisons of six 5-iodonucleosides. Nuclear Medicine and Biology, 2003, 30, 687-696.	0.6	22
35	Comparison of conventional and novel PET tracers for imaging mesothelioma in nude mice with subcutaneous and intrapleural xenografts. Nuclear Medicine and Biology, 2009, 36, 379-388.	0.6	21
36	Basal μ-opioid receptor availability in the amygdala predicts the inhibition of pain-related brain activity during heterotopic noxious counter-stimulation. Neuroscience Research, 2014, 81-82, 78-84.	1.9	21

#	Article	IF	CITATIONS
37	Alkyl-fluorinated thymidine derivatives for imaging cell proliferation. Nuclear Medicine and Biology, 2006, 33, 765-772.	0.6	20
38	Preclinical and the first clinical studies on [11C]ITMM for mapping metabotropic glutamate receptor subtype 1 by positron emission tomography. Nuclear Medicine and Biology, 2013, 40, 214-220.	0.6	20
39	Evaluation of 4′-[Methyl-11C]Thiothymidine in a Rodent Tumor and Inflammation Model. Journal of Nuclear Medicine, 2012, 53, 488-494.	5.0	19
40	18F-THK5351 PET Can Identify Astrogliosis in Multiple Sclerosis Plaques. Clinical Nuclear Medicine, 2020, 45, e98-e100.	1.3	19
41	Differential effects of age on human striatal adenosine A ₁ and A _{2A} receptors. Synapse, 2012, 66, 832-839.	1.2	18
42	Radiosynthesis and in vivo evaluation of two imidazopyridineacetamides, [11C]CB184 and [11C]CB190, as a PET tracer for 18ÂkDa translocator protein: direct comparison with [11C](R)-PK11195. Annals of Nuclear Medicine, 2015, 29, 325-335.	2.2	17
43	Comparison of 4′-[methyl-11C]thiothymidine (11C-4DST) and 3′-deoxy-3′-[18F]fluorothymidine (18F-FL ⁻ PET/CT in human brain glioma imaging. EJNMMI Research, 2015, 5, 7.	Г) _{2.5}	16
44	Characterization of the binding of tau imaging ligands to melanin-containing cells: putative off-target-binding site. Annals of Nuclear Medicine, 2019, 33, 375-382.	2.2	16
45	A pilot study of 4′-[methyl-11C]-thiothymidine PET/CT for detection of regional lymph node metastasis in non-small cell lung cancer. EJNMMI Research, 2014, 4, 10.	2.5	15
46	Monoamine Oxidase B Binding of 18F-THK5351 to Visualize Glioblastoma and Associated Gliosis. Clinical Nuclear Medicine, 2019, 44, 507-509.	1.3	15
47	Head-to-Head Comparison of the Two MAO-B Radioligands, 18F-THK5351 and 11C-L-Deprenyl, to Visualize Astrogliosis in Patients With Neurological Disorders. Clinical Nuclear Medicine, 2021, 46, e31-e33.	1.3	15
48	Alkyl-fluorinated thymidine derivatives for imaging cell proliferation. Nuclear Medicine and Biology, 2006, 33, 751-764.	0.6	14
49	Volumetric comparison of positron emission tomography/computed tomography using 4′-[methyl-11C]-thiothymidine with 2-deoxy-2-18F-fluoro-D-glucose in patients with advanced head and neck squamous cell carcinoma. Nuclear Medicine Communications, 2015, 36, 219-225.	1.1	14
50	Evaluation of [11C]CB184 for imaging and quantification of TSPO overexpression in a rat model of herpes encephalitis. European Journal of Nuclear Medicine and Molecular Imaging, 2015, 42, 1106-1118.	6.4	14
51	Correlation of 4′-[methyl-11C]-thiothymidine uptake with Ki-67 immunohistochemistry and tumor grade in patients with newly diagnosed gliomas in comparison with 11C-methionine uptake. Annals of Nuclear Medicine, 2016, 30, 89-96.	2.2	14
52	Pharmacokinetic Modeling of [18F]MC225 for Quantification of the P-Glycoprotein Function at the Blood–Brain Barrier in Non-Human Primates with PET. Molecular Pharmaceutics, 2020, 17, 3477-3486.	4.6	14
53	11C-Labeled Analogs of Indomethacin Esters and Amides for Brain Cyclooxygenase-2 Imaging: Radiosynthesis, in Vitro Evaluation and in Vivo Characteristics in Mice. Chemical and Pharmaceutical Bulletin, 2011, 59, 938-946.	1.3	13
54	Pharmacokinetics and metabolism of 5-125I-iodo-4'-thio-2'-deoxyuridine in rodents. Journal of Nuclear Medicine, 2003, 44, 1671-6.	5.0	13

#	Article	IF	CITATIONS
55	Development of PET radiopharmaceuticals and their clinical applications at the Positron Medical Center. Geriatrics and Gerontology International, 2010, 10, S180-96.	1.5	12
56	In vivo evaluation of carbon-11-labelled non-sarcosine-based glycine transporter 1 inhibitors in mice and conscious monkeys. Nuclear Medicine and Biology, 2011, 38, 517-527.	0.6	12
57	Re-evaluation of in vivo selectivity of [11C]SA4503 to Ïf1 receptors in the brain: Contributions of emopamil binding protein. Nuclear Medicine and Biology, 2012, 39, 1049-1052.	0.6	12
58	Longitudinal observation of [11C]4DST uptake in turpentine-induced inflammatory tissue. Nuclear Medicine and Biology, 2013, 40, 240-244.	0.6	12
59	In vitro analysis of transport and metabolism of 4′-thiothymidine in human tumor cells. Nuclear Medicine and Biology, 2015, 42, 470-474.	0.6	12
60	Comparison of 11C-4DST and 18F-FDG PET/CT imaging for advanced renal cell carcinoma: preliminary study. Abdominal Radiology, 2016, 41, 521-530.	2.1	12
61	Relationship between type 1 metabotropic glutamate receptors and cerebellar ataxia. Journal of Neurology, 2016, 263, 2179-2187.	3.6	12
62	Unchanged type 1 metabotropic glutamate receptor availability in patients with Alzheimer's disease: A study using 11C-ITMM positron emission tomography. NeuroImage: Clinical, 2019, 22, 101783.	2.7	12
63	Animal tumor models for PET in drug development. Annals of Nuclear Medicine, 2011, 25, 717-731.	2.2	11
64	Comparison of imaging using 11 C-ITMM and 18 F-FDG for the detection of cerebellar ataxia. Journal of the Neurological Sciences, 2017, 375, 97-102.	0.6	11
65	Pharmacological characterization of [1251]CHIBA-1006 binding, a new radioligand for α7 nicotinic acetylcholine receptors, to rat brain membranes. Brain Research, 2010, 1360, 130-137.	2.2	10
66	Preclinical and first-in-man studies of [11C]CB184 for imaging the 18-kDa translocator protein by positron emission tomography. Annals of Nuclear Medicine, 2016, 30, 534-543.	2.2	10
67	18F-FDG and 11C-4DST PET/CT for evaluating response to platinum-based doublet chemotherapy in advanced non-small cell lung cancer: a prospective study. EJNMMI Research, 2019, 9, 4.	2.5	10
68	Metabolic Network Topology of Alzheimer's Disease and Dementia with Lewy Bodies Generated Using Fluorodeoxyglucose Positron Emission Tomography. Journal of Alzheimer's Disease, 2020, 73, 197-207.	2.6	10
69	Relationship between the temporal course of astrogliosis and symptom improvement in cerebral infarction: report of a case monitored using 18F-THK5351 positron emission tomography. BMC Medical Imaging, 2020, 20, 81.	2.7	10
70	Mechanical Regulation Underlies Effects of Exercise on Serotonin-Induced Signaling in the Prefrontal Cortex Neurons. IScience, 2020, 23, 100874.	4.1	10
71	Adenosine <scp>A_{2A}</scp> Receptor Occupancy by Caffeine After Coffee Intake in Parkinson's Disease. Movement Disorders, 2022, 37, 853-857.	3.9	10
72	Acquisition of resistance to antitumor alkylating agent ACNU: a possible target of positron emission tomography monitoring. Nuclear Medicine and Biology, 2006, 33, 29-35.	0.6	9

#	Article	IF	CITATIONS
73	Age-Related Decrease in Male Extra-Striatal Adenosine A1 Receptors Measured Using11C-MPDX PET. Frontiers in Pharmacology, 2017, 8, 903.	3.5	9
74	Response of Cerebral Blood Flow and Blood Pressure to Dynamic Exercise: A Study Using PET. International Journal of Sports Medicine, 2018, 39, 181-188.	1.7	9
75	Increased Binding Potential of Brain Adenosine A ₁ Receptor in Chronic Stages of Patients with Diffuse Axonal Injury Measured with [1-methyl- ¹¹ C] 8-dicyclopropylmethyl-1-methyl-3-propylxanthine Positron Emission Tomography Imaging. Journal of Neurotrauma. 2018. 35. 25-31.	3.4	9
76	A pitfall of white matter reference regions used in [18F] florbetapir PET: a consideration of kinetics. Annals of Nuclear Medicine, 2019, 33, 848-854.	2.2	9
77	Pharmacological Characterization of [3H]CHIBA-3007 Binding to Glycine Transporter 1 in the Rat Brain. PLoS ONE, 2011, 6, e21322.	2.5	9
78	PET Imaging of ¹⁸ F-FDC, ¹¹ C-methionine, ¹¹ C-flumazenil, and ¹¹ C-4DST in Progressive Multifocal Leukoencephalopathy. Internal Medicine, 2017, 56, 1219-1223.	0.7	9
79	Reliable radiosynthesis of 4-[10B]borono-2-[18F]fluoro-l-phenylalanine with quality assurance for boron neutron capture therapy-oriented diagnosis. Annals of Nuclear Medicine, 2018, 32, 463-473.	2.2	8
80	Efficacy of 4′-[methyl-11C] thiothymidine PET/CT before and after neoadjuvant therapy for predicting therapeutic responses in patients with esophageal cancer: a pilot study. EJNMMI Research, 2019, 9, 10.	2.5	8
81	Preclinical Evaluation of an ¹⁸ F-Labeled SW-100 Derivative for PET Imaging of Histone Deacetylase 6 in the Brain. ACS Chemical Neuroscience, 2021, 12, 746-755.	3.5	8
82	Determination of optimal regularization factor in Bayesian penalized likelihood reconstruction of brain PET images using [¹⁸ F]FDG and [¹¹ C]PiB. Medical Physics, 2022, 49, 2995-3005.	3.0	8
83	Distribution Pattern of the Monoamine Oxidase B Ligand, 18F-THK5351, in the Healthy Brain. Clinical Nuclear Medicine, 2022, 47, e489-e495.	1.3	8
84	Synthesis and evaluation of 7α-(3-[18F]fluoropropyl) estradiol. Nuclear Medicine and Biology, 2015, 42, 590-597.	0.6	7
85	Evaluation of peri-implant bone metabolism under immediate loading using high-resolution Na18F-PET. Clinical Oral Investigations, 2017, 21, 2029-2037.	3.0	7
86	Dynamic Exercise Elicits Dissociated Changes Between Tissue Oxygenation and Cerebral Blood Flow in the Prefrontal Cortex: A Study Using NIRS and PET. Advances in Experimental Medicine and Biology, 2018, 1072, 269-274.	1.6	7
87	Evaluation of P-glycoprotein function at the blood–brain barrier using [18F]MC225-PET. European Journal of Nuclear Medicine and Molecular Imaging, 2021, 48, 4105-4106.	6.4	7
88	Importance of P-gp PET Imaging in Pharmacology. Current Pharmaceutical Design, 2016, 22, 5830-5836.	1.9	7
89	Age and gender effects of 11C-ITMM binding to metabotropic glutamate receptor type 1 in healthy human participants. Neurobiology of Aging, 2017, 55, 72-77.	3.1	6
90	Assessment of safety, efficacy, and dosimetry of a novel 18-kDa translocator protein ligand, [11C]CB184, in healthy human volunteers. EJNMMI Research, 2017, 7, 26.	2.5	6

#	Article	IF	CITATIONS
91	Effects of a novel tungsten-impregnated rubber neck shield on the quality of cerebral images acquired using 15O-labeled gas. Radiological Physics and Technology, 2017, 10, 422-430.	1.9	6
92	4′-[methyl-11C]-thiothymidine as a proliferation imaging tracer for detection of colorectal cancer: comparison with 18F-FDG. Annals of Nuclear Medicine, 2019, 33, 822-827.	2.2	6
93	Effects of 18F-fluorinated neopentyl glycol side-chain on the biological characteristics of stilbene amyloid-β PET ligands. Nuclear Medicine and Biology, 2021, 94-95, 38-45.	0.6	6
94	Head-to-head comparison of (R)-[11C]verapamil and [18F]MC225 in non-human primates, tracers for measuring P-glycoprotein function. European Journal of Nuclear Medicine and Molecular Imaging, 2021, 48, 4307-4317.	6.4	6
95	<i>Nâ€</i> Alkyl 3â€aminobutâ€2â€enenitrile as a Nonâ€radioactive Side Product in Nucleophilic ¹⁸ Fâ€Fluorination. ChemistrySelect, 2021, 6, 2826-2831.	1.5	5
96	Automated synthesis, preclinical toxicity, and radiation dosimetry of [18F]MC225 for clinical use: a tracer for measuring P-glycoprotein function at the blood-brain barrier. EJNMMI Research, 2020, 10, 84.	2.5	5
97	Evaluation of DNA synthesis with carbon-11-labeled 4′-thiothymidine. World Journal of Radiology, 2016, 8, 799.	1.1	5
98	Application of [11C]SA4503 to selection of novel $if1$ selective agonists. Nuclear Medicine and Biology, 2012, 39, 1117-1121.	0.6	4
99	Differential human brain activity induced by two perceptually indistinguishable gentle cutaneous stimuli. NeuroReport, 2013, 24, 425-430.	1.2	4
100	Microglial Activation on 11C-CB184 PET in a Patient With Cerebellar Ataxia Associated With HIV Infection. Clinical Nuclear Medicine, 2018, 43, e82-e84.	1.3	4
101	Searching for diagnostic properties of novel fluorine-18-labeled d-allose. Annals of Nuclear Medicine, 2019, 33, 855-865.	2.2	4
102	Radiosynthesis and preliminary evaluation of an ¹⁸ Fâ€labeled tubastatin A analog for PET imaging of histone deacetylase 6. Journal of Labelled Compounds and Radiopharmaceuticals, 2020, 63, 85-95.	1.0	4
103	Automated production of [18F]MK-6240 on CFN-MPS200. Applied Radiation and Isotopes, 2021, 168, 109468.	1.5	4
104	Radiosynthesis and <i>in Vivo</i> and <i>ex Vivo</i> Evaluation of Isomeric [¹¹ C]methoxy Analogs of Nimesulide as Brain Cyclooxygenase-2-Targeted Imaging Agents. Biological and Pharmaceutical Bulletin, 2022, 45, 94-103.	1.4	4
105	Comparison of dosimetry between PET/CT and PET alone using 11C-ITMM. Australasian Physical and Engineering Sciences in Medicine, 2016, 39, 177-186.	1.3	3
106	(R)-[11C]Emopamil as a novel tracer for imaging enhanced P-glycoprotein function. Nuclear Medicine and Biology, 2016, 43, 52-62.	0.6	3
107	Adenosine <scp>A_{2A}</scp> Receptor Occupancy by Longâ€Term Istradefylline Administration in Parkinson's Disease. Movement Disorders, 2021, 36, 268-269.	3.9	3
108	Pharmacokinetic Modeling of (<i>R</i>)-[¹¹ C]verapamil to Measure the P-Glycoprotein Function in Nonhuman Primates. Molecular Pharmaceutics, 2021, 18, 416-428.	4.6	3

0

#	Article	IF	CITATIONS
109	Determination of radionuclides and radiochemical impurities produced by in-house cyclotron irradiation and subsequent radiosynthesis of PET tracers. Annals of Nuclear Medicine, 2017, 31, 84-92.	2.2	2
110	Correlation of 4′-[methyl-11C]-thiothymidine uptake with human equilibrative nucleoside transporter-1 and thymidine kinase-1 expressions in patients with newly diagnosed gliomas. Annals of Nuclear Medicine, 2018, 32, 634-641.	2.2	2
111	Interim 4′-[methyl-11C]-thiothymidine PET for predicting the chemoradiotherapeutic response in head and neck squamous cell carcinoma: comparison with [18F]FDG PET. EJNMMI Research, 2021, 11, 13.	2.5	2
112	Efficacy of cell proliferation imaging with 4DST PET/CT for predicting the prognosis of patients with esophageal cancer: a comparison study with FDG PET/CT. European Journal of Nuclear Medicine and Molecular Imaging, 2021, 48, 2615-2623.	6.4	2
113	In Vivo Evaluation of11C-labeled Three Radioligands for Glycine Transporter 1 in the Mouse Brain. Clinical Psychopharmacology and Neuroscience, 2012, 10, 34-43.	2.0	2
114	Use of 11C-4DST-PET for Imaging of Human Brain Tumors. Tumors of the Central Nervous System, 2014, , 41-48.	0.1	2
115	Synthesis and evaluation of N-isopropyl-p-[11C]methylamphetamine as a novel cerebral blood flow tracer for positron emission tomography. EJNMMI Research, 2020, 10, 115.	2.5	2
116	Texture indices of 4â€2-[methyl-11C]-thiothymidine uptake predict p16 status in patients with newly diagnosed oropharyngeal squamous cell carcinoma: comparison with 18F-FDG uptake. European Journal of Hybrid Imaging, 2020, 4, 20.	1.5	2
117	Roles of $if1$ receptors in the mechanisms of action of CNS drugs. Translational Neuroscience, 2012, 3, .	1.4	1
118	Optimization of the alkyl side chain length of fluorine-18-labeled 7α-alkyl-fluoroestradiol. Nuclear Medicine and Biology, 2016, 43, 512-519.	0.6	1
119	Synthesis and basic evaluation of 7α-(3-[18F]fluoropropyl)-testosterone and 7α-(3-[18F]fluoropropyl)-dihydrotestosterone. Annals of Nuclear Medicine, 2017, 31, 53-62.	2.2	1
120	Density of metabotropic glutamate receptors subtype 1 in Parkinson's disease compared to healthy elderly – a ITMM PET study –. Journal of the Neurological Sciences, 2017, 381, 806-807.	0.6	1
121	Usefulness of ¹¹ C-Methionine Positron Emission Tomography for Monitoring of Treatment Response and Recurrence in a Clioblastoma Patient on Bevacizumab Therapy: A Case Report. Case Reports in Oncology, 2018, 11, 442-449.	0.7	1
122	Radiosynthesis of 18F-labeled d-allose. Carbohydrate Research, 2019, 486, 107827.	2.3	1
123	Preâ€discard estimation of radioactivated materials in positron emission tomography cyclotron systems and concrete walls of a cyclotron vault. Medical Physics, 2019, 46, 2457-2467.	3.0	1
124	Correlation of 4â€2-[methyl-11C]-thiothymidine PET with Gd-enhanced and FLAIR MRI in patients with newly diagnosed glioma. EJNMMI Research, 2021, 11, 42.	2.5	1
125	PET Imaging of Sigma1 Receptors. , 2014, , 741-763.		1

Brain Imaging of Sigma Receptors. , 2014, , 99-112.

#	Article	IF	CITATIONS
127	Human Brain Imaging of Acetylcholine Receptors. , 2014, , 113-160.		0
128	PET imaging for altered brain function evoked by exercise: measurements of changes in cerebral blood flow and neurotransmitters. No Junkan Taisha = Cerebral Blood Flow and Metabolism, 2017, 28, 297-302.	0.0	0
129	Validation of scatter limitation correction to eliminate scatter correction error in oxygen-15 gas-inhalation positron emission tomography images. Nuclear Medicine Communications, 2018, 39, 936-944.	1.1	0
130	Correlation of 4′-[methyl-11C]-thiothymidine PET with Ki-67 immunohistochemistry separately in patients with newly diagnosed and recurrent gliomas. Nuclear Medicine Communications, 2021, Publish Ahead of Print, 1322-1327.	1.1	0
131	First clinical assessment of [18F]MC225, a novel fluorine-18 labelled PET tracer for measuring functional P-glycoprotein at the blood–brain barrier. Annals of Nuclear Medicine, 2021, 35, 1240-1252.	2.2	0
132	Test–retest reproducibility of cerebral adenosine A2A receptor quantification using [11C]preladenant. Annals of Nuclear Medicine, 2022, 36, 15-23.	2.2	0
133	Cerebral Blood Flow during Dynamic Exercise Correlates with Blood Pressure in Autonomic Brain Regions. Medicine and Science in Sports and Exercise, 2017, 49, 824.	0.4	0
134	Voxel-based morphometry focusing on medial temporal lobe structures has a limited capability to detect amyloid β, an Alzheimer's disease pathology. Aging, 2020, 12, 19701-19710.	3.1	0